

Distortion-sensitive insight into the pretransitional behavior of 4-*n*-octyloxy-4'-cyanobiphenyl (8OCB)

This content has been downloaded from IOPscience. Please scroll down to see the full text.

2013 J. Phys.: Condens. Matter 25 245105

(<http://iopscience.iop.org/0953-8984/25/24/245105>)

View [the table of contents for this issue](#), or go to the [journal homepage](#) for more

Download details:

IP Address: 130.92.9.57

This content was downloaded on 04/04/2014 at 21:51

Please note that [terms and conditions](#) apply.

Distortion-sensitive insight into the pretransitional behavior of 4-*n*-octyloxy-4'-cyanobiphenyl (8OCB)

Sylwester J Rzoska^{1,2}, Aleksandra Drozd-Rzoska³, Prabir K Mukherjee⁴, David O Lopez^{5,6} and Julio C Martinez-Garcia⁷

¹ Institute of Physics, University of Silesia, Uniwersytecka 4, 40-007 Katowice, Poland

² Institute of High Pressure Physics PAS, Sokołowska 29/37, 00-142 Warsaw, Poland

³ Foundation C2B, ulica Wolności 3/5, 41-500 Chorzów, Poland

⁴ Department of Physics, Government College of Engineering and Textile Technology, 12 William Carey Road, Serampore, Hooghly-712201, India

⁵ Grup de Propietas Físiques dels Materials, Departament de Física i Enginyeria Nuclear, Universitat Politècnica de Catalunya, Diagonal 647, E-08028 Barcelona, Spain

⁶ Departamento de Física Aplicada II, Facultad de Ciencia y Tecnología, Universidad del País Vasco, Apartado 644, E-48080 Bilbao, Spain

⁷ Department of Chemistry and Biochemistry, University of Berne, Freiestrasse 3, CH-3012 Berne, Switzerland

E-mail: sylwester.rzoska@gmail.com


Received 25 November 2012, in final form 12 April 2013

Published 29 May 2013

Online at stacks.iop.org/JPhysCM/25/245105

Abstract


Results of studies of the static and dynamic dielectric properties in rod-like 4-*n*-octyloxy-4'-cyanobiphenyl (8OCB) with isotropic (I)–nematic (N)–smectic A (SmA)–crystal (Cr) mesomorphism, combined with measurements of the low-frequency nonlinear dielectric effect and heat capacity are presented. The analysis is supported by the derivative-based and distortion-sensitive transformation of experimental data. Evidence for the I–N and N–SmA pretransitional anomalies, indicating the influence of tricritical behavior, is shown. It has also been found that neither the N phase nor the SmA phase are uniform and hallmarks of fluid–fluid crossovers can be detected. The dynamics, tested via the evolution of the primary relaxation time, is clearly non-Arrhenius and described via $\tau(T) = \tau_c(T - T_C)^{-\phi}$. In the immediate vicinity of the I–N transition a novel anomaly has been found: $\Delta\tau \propto 1/(T - T^*)$, where T^* is the temperature of the virtual continuous transition and $\Delta\tau$ is the excess over the ‘background behavior’. Experimental results are confronted with the comprehensive Landau–de Gennes theory based modeling.

 Online supplementary data available from stacks.iop.org/JPhysCM/25/245105/mmedia

(Some figures may appear in colour only in the online journal)

1. Introduction

Soft matter systems are recognized as one of the key challenges of twenty-first century condensed matter physics,

 Content from this work may be used under the terms of the [Creative Commons Attribution 3.0 licence](http://creativecommons.org/licenses/by/3.0/). Any further distribution of this work must maintain attribution to the author(s) and the title of the work, journal citation and DOI.

biophysics, material engineering, and food science [1–4]. Soft matter systems are associated with several common features: (i) the basic importance of mesoscale structures and processes, (ii) complex dynamics, (iii) high sensitivity to external perturbations and (iv) the richness of phase transitions. Liquid crystals (LC) fulfil these conditions in a model way. The most ‘classical’ topic in this field is the physics of thermotropic rod-like liquid crystals. However, even for this

mature area basic features are surprisingly puzzling. This applies in particular to the characteristics of phase transitions, parameterizations of dynamic features or the fragmentation into static, thermodynamic and dynamic insights [5–17]. Notable also are emerging links with apparently distinct soft matter systems, such as supercooled glass-forming liquids [14–18].

Recent studies of soft matter systems showed that the implementation of the derivative-based and distortion-sensitive preliminary transformation of experimental data can reveal novel features poorly manifested in the direct fit of experimental data. Such an analysis also enables a reliable estimation of the optimal values of key parameters and the domain of validity of a given type of description [13–18]. In this paper such a methodology has been employed for the analysis of the evolution of the static dielectric permittivity, low-frequency nonlinear dielectric effect (LF NDE), heat capacity and primary dielectric relaxation time in a rod-like liquid crystalline (LC) material with isotropic–nematic–smectic A (SmA) mesomorphism.

In the subsequent sections, firstly significant experimental characteristics are recalled. Next, the derivative-based analysis of experimental data is presented. Subsequently, the comprehensive Landau–de Gennes modeling of both I–N and N–SmA transitions is shown. Finally, all these techniques are employed and confronted with the results of experimental studies in *n*-octyloxycyanobiphenyl (8OCB), one of the most ‘classical’ rod-like compounds.

Critical summary of existing experimental evidence.

There are several theoretical concepts used in describing phase transitions in rod-like LC materials, however, the most important is probably the Landau–de Gennes (LdG) model [5–10]. Its first great success was the parameterization of strong pretransitional anomalies of the Kerr effect (KE), the Cotton–Mouton effect (CME) and the intensity of scattered light (I_L) in the isotropic phase [19–29]:

$$I_L, KE, CME \propto \frac{A_{\text{method}}}{(T - T^*)^\gamma}, \quad \text{for } T > T^C = T^* + \Delta T^* \quad (1)$$

where the exponent $\gamma = 1$ is related to the pretransitional anomaly of compressibility (susceptibility), T^* denotes the extrapolated temperature of a hypothetical (virtual) continuous phase transition and $\Delta T^* = T_{\text{IN}} - T^*$ is a measure of the discontinuity of the I–N transition: usually $\Delta T^* = 1\text{--}2$ K. $T^C = T_{\text{IN}}$ stands for the I–N orientational melting temperature (clearing temperature). The coefficient A_{method} depends on the amplitude of the pretransitional anomaly of compressibility and molecular anisotropies linked to the KE, CME or I_L .

This equation appears to be valid also for the low-frequency nonlinear dielectric effect (LF NDE), where small changes of dielectric permittivity $\Delta \epsilon^E$ induced by the strong electric field are detected by a weak radio-frequency electric field whose frequency fulfils the condition $\tau_{\text{sampling}} = 1/f_{\text{sampling}} \gg \tau_{\text{fluct.}}(T_{\text{IN}})$ [30, 31]. The latter denotes the relaxation time of prenematic fluctuations in the isotropic

phase [8]:

$$\tau_{\text{fluct.}} \propto \frac{1}{(T - T^*)^{z\nu}} \quad T > T^C \text{ and } \nu = 1/2, z = 2 \quad (2)$$

where z is the dynamical exponent and for typical LC rod-like material, $\tau_{\text{fluct.}}(T_{\text{IN}}) \sim 1 \mu\text{s}$.

In the case of KE, CME and I_L , the detection is associated with the frequency of light: $1/f_{\text{sampling}} \ll \tau_{\text{fluct.}}(T_{\text{IN}})$. It is noteworthy that for these methods careful studies always reveal significant deviations from equation (1) in the immediate vicinity of the clearing temperature. Beyond the simplest case of the I–N transition they are so strong that there are still no reliable proposals for parameterizations in this case. The unique feature of LF NDE is the validity of equation (1) without any deviations near the clearing temperature for the I–N, I–SmA, I–Chiral Nematic (N^*) and I–Smectic E (I–SmE) transitions [30, 31]. This may be associated with the mentioned qualitative difference between time scales for KE, CME, I_L and LF NDE.

LF NDE may be considered as the ‘static nonlinear dielectric permittivity’, coupled directly to multimolecular pretransitional fluctuations. The ‘static linear, dielectric permittivity’ (dielectric constant, ϵ') also exhibits a pretransitional anomaly, but it is linked to an averaged single molecule. For rod-like compounds with a permanent dipole moment approximately parallel to the long axis of an LC molecule this anomaly can be described by [32–34]:

$$\epsilon'(T) = \epsilon'^* + a_{\text{Iso}} \Delta \tilde{T} + A_{\text{Iso}} (\Delta \tilde{T})^{1-\alpha} \quad (3)$$

where $\Delta \tilde{T} = (T - T^*)/T^*$ is the normalized temperature distance from the virtual continuous phase transition. The locus of this transition is given by (ϵ^*, T^*) .

On cooling towards the clearing temperature the number of molecules within the prenematic fluctuations increases. The characteristic for the nematic phase equivalence of \mathbf{n} and $-\mathbf{n}$ directors causes the cancellation of permanent dipole moments ordered in an antiparallel way within the fluctuations. Consequently the static permittivity within the fluctuations is much smaller than for the fluid-like surroundings. This causes a crossover from the domain characterized by $d\epsilon'/dT < 0$ to $d\epsilon'/dT > 0$ on approaching the clearing temperature.

A similar equation governs the pretransitional anomaly of density, although it is qualitatively weaker than for $\epsilon'(T)$ [8, 35, 36]:

$$\rho(T) = \rho^* + r_1 \Delta \tilde{T} + R (\Delta \tilde{T})^{1-\alpha}. \quad (4)$$

For the heat capacity in the isotropic phase of nematogens [7, 8, 37–40]:

$$C_P^+(T) = b + a^+ \Delta \tilde{T} + A^+ (\Delta \tilde{T})^{-\alpha}. \quad (5)$$

Relations similar to equations (4) and (5) are valid also in the nematic phase, below the I–N transition. In this case, $\Delta \tilde{T} = (T^{**} - T)/T^{**}$, where T^{**} stands for the ‘mirror’ of the hypothetical continuous phase transition in the isotropic phase [7, 8, 37–40].

The fundamental characteristic of a continuous phase transition is the order parameter $S(T)$, describing the degree

of appearance/disappearance of an element of symmetry [7]. In the nematic phase it can be estimated from the anisotropy of the refractive index ($n^{\parallel} - n^{\perp}$) or the static dielectric permittivity ($\varepsilon^{\parallel} - \varepsilon^{\perp}$), where indices \parallel and \perp indicate the parallel and perpendicular orientation of rod-like molecules [5–10]. To describe its temperature dependence, the empirical Haller formula is often used [6, 8, 41–46]:

$$S(T) = S_0 |T - T^+|^{\beta'} \quad (6)$$

where T^+ is linked to the clearing temperature (T^C) or its vicinity, and the empirical power exponent $\beta' = 0.1$ – 0.2 .

However, this relation cannot describe the immediate vicinity of the I–N transition and has a limited physical meaning. More justified is the relation which can be derived from the LdG model, namely [5–8]:

$$S(T) = S^{**} + S_0 |T^{**} - T|^{\beta}. \quad (7)$$

Fittings of experimental data gave $\beta = 0.25$ – 0.5 , i.e. values ranging between the basic LdG model value ($\beta = 1/2, d = 4$, where d is the space dimensionality), and the tricritical point (TCP) extension ($\beta = 1/4, d = 3$). S^{**} and T^{**} are the values of the order parameter and temperature for the terminus of the superheated nematic phase.

On cooling, the nematic phase may be followed by the additionally 1D translationally ordered, layered, SmA mesophase. So far, one of the key pieces of experimental evidence for this domain is associated with the heat capacity scan, namely [5–12, 38–40, 47, 48]:

$$C_p^{\pm}(T) = C + a\Delta\tilde{T} + A_{\text{NA}}^{\pm} (\Delta\tilde{T})^{-\alpha} (1 + D^{\pm} (\Delta\tilde{T})^{0.5}) \quad (8)$$

where ‘ \pm ’ stands for the nematic and the smectic mesophase, respectively, and the term in brackets is a correction-to-scaling term significant for non-mean-field behavior when moving away from the ‘critical’ point.

De Gennes noted the similarity of the N–SmA transition to the metal–superconductor transition [5]. Consequently, this transition should belong to the 3D XY universality class with an exponent $\alpha \approx -0.07$ [5–8]. In practice, the value of α ranges between 3D XY (-0.07) and tricritical ($1/2$) values in various LC systems [8, 10, 12, 38–40, 47, 48]. This unusual situation still lacks a definitive explanation. Also puzzling is the question of the ‘general’ pattern of the order of this transition (continuous or discontinuous). The evidence related to the manifestation of the pretransitional behavior of dielectric properties for the N–SmA transition is still very limited ([40] and references therein).

Surprisingly, despite decades of extensive studies there is still inconclusive evidence of the evolution of basic dynamic properties in LC materials. Generally, one can expect analogous behavior of the viscosity, diffusion coefficient or primary relaxation time. The latter is particularly convenient for high-resolution tests due to enormous possibilities of modern broad band dielectric spectroscopy (BDS) [49]. The vast majority of reports indicate a simple Arrhenius behavior $\tau(T) = \tau_0 \exp(E_a/kT)$, where $E_a = \text{const}$ stands for the activation energy [6, 8, 10–12, 42, 43]. However, even three decades ago Diogo and Martins suggested an

‘apparent’ form of the activation energy, depending on the order parameter [50]:

$$\tau(T) = \tau_0 \frac{kT}{h} \exp\left(\frac{\varepsilon S}{kT}\right) \exp\left(\frac{\Theta S^2}{T - T_0}\right) \quad (9)$$

where k, h, Θ and T_0 are empirical adjustable parameters.

According to Diogo and Martins this can be reduced to Arrhenius behavior if the first exponential term dominates. Otherwise it takes the Vogel–Fulcher–Tammann (VFT) form, namely [50, 51]:

$$\tau(T) = \tau_0 \exp\left(\frac{B}{T - T_0}\right) = \tau_0 \exp\left(\frac{\Theta S^2}{T - T_0}\right) \quad (10)$$

where the right hand of this relation is the basic VFT equation.

Recalling the VFT notation developed for supercooled glass-forming liquids, $B = D_T T_0$, where D_T is the fragility strength coefficient, a value that indicates the discrepancy from the simple Arrhenius pattern, and T_0 is the estimation of the ideal glass transition, located well below the hypothetical glass temperature ($T_0 \ll T_g$) [49]. To the best of the given authors knowledge in implementations of equation (10) the temperature dependence of $S(T)$ has hardly been used, but there are studies for supercooled n -alkylcyanobiphenyls (n CBs) showing the parameterization via the VFT equation [16, 52, 53]. However, in the past decade, experiments in n CBs clearly proved a limited adequacy of the VFT equation and the superior features of the critical-like description [15–17]:

$$\tau(T) = \tau_C \left(\frac{T - T_X}{T_X}\right)^{-\phi} \quad (11)$$

where $T_X < T_g$ ($\tau(T_g) = 100$ s).

Such a description in the isotropic phase of n CBs gave $T_X \approx T^C - 30$ K, $\tau(T_X) \approx 10^{-7}$ s and $\phi = 1.5$ – 2.5 [14–17]. It agrees well with the mode coupling theory predictions. In the ultraviscous domain for $\tau > \tau(T_X) \approx 10^{-7}$ s one obtains $T_X \approx T_C = T_g - 10$ K and $\phi \approx 9$. Such behavior supports the possible link between the dynamics of isotropic LC and glass-forming liquids, suggested theoretically [49, 14–17]. In this paper, issues related to the distribution of relaxation time and the decoupling between translational and orientational degrees of freedom are not studied. Recent advances related to these topics are presented in [17, 54, 55].

Derivative-based and distortion-sensitive analysis.

In [14] the linearized, derivative-based analysis for testing the appearance of the Arrhenius or the non-Arrhenius temperature behavior of the primary relaxation time or viscosity in soft matter systems was analyzed. Generally, the non-Arrhenius temperature behavior is described by:

$$\tau(T) = \tau_0 \exp\left(\frac{E_a(T)}{RT}\right) \quad (12)$$

where $E_a(T)$ is the apparent (temperature-dependent) activation energy: for the basic Arrhenius behavior $E_a(T) = E_a = \text{const}$. and R stands for the gas constant.

Linking the above equation with the VFT relation one obtains [14]:

$$\begin{aligned} \left[\frac{d \ln \tau}{d(1/T)} \right]^{-1/2} &= \frac{H_a(1/T)}{R} = [H'_a(1/T)]^{-1/2} \\ &= [(D_T T_0)^{-1/2}] - \frac{[T_0(D_T T_0)^{-1/2}]}{T} \\ &= B - \frac{A}{T} \end{aligned} \quad (13)$$

where $H'_a(T)$ stands for the normalized apparent enthalpy.

For the critical-like equation (11) one can derive [14, 15]:

$$\frac{T^2}{H'_a(T)} = \frac{T - T_C}{\phi} = AT - B. \quad (14)$$

For plots exploring equations (13) or (14), regions where $\tau(T)$ evolution is associated with the simple Arrhenius equation are indicated by the horizontal linear behavior. Regions in which the VFT (equations (10) and (13)) or the critical-like (equations (11) and (14)) parameterization can be applied are indicated by sloped linear domains. The subsequent linear regression analysis can yield optimal values for the basic parameters. Consequently, the final fitting via equation (10) or (11) can be reduced solely to τ_0 or τ_C prefactors in the clearly pre-identified temperature domains.

Derivative-based analysis may be also employed for static physical properties. In this case it allows one to reduce the number of fitted parameters and ultimately indicate the region where the given type of description can be applied. In [13, 30] it was employed in supporting analysis of the static dielectric permittivity (equation (3)), yielding:

$$\frac{d\varepsilon'}{dT} = a_{\text{Iso}}T + (1 - \alpha)A_{\text{Iso}}(\Delta\tilde{T})^{-\alpha}. \quad (15)$$

In [16, 17, 30] the analysis of $d\varepsilon'/dT$ versus T in the isotropic phase yielded amplitudes and exponents, which when substituted into equation (3) led to superior $\varepsilon'(T)$ parameterization.

In this paper such a supporting procedure is used both for the I–N and N–SmA transitions.

The analysis of experimental data via a $d\varepsilon'/dT$ versus T plot makes it also possible to detect subtle changes in preferences of parallel/antiparallel ordering of permanent dipole moments, hardly visible for the basic $\varepsilon'(T)$ plot. Derivative-based analysis seems to be particularly important for optimal parameterization of the order parameters. Although equation (7) seems to be simple, its implementation is difficult since the most characteristic part of $S(T)$ behavior is not available due to the discontinuous character of the I–N transition. However, one can consider the following transformation of experimental data [13]:

$$\frac{dS}{dT} = \beta S_0 (T^{**} - T)^{\beta-1}. \quad (16)$$

Consequently, for the plot $\log_{10}(dS/dT)$ versus $\log(T^{**} - T)$ one obtains linear behavior for the optimal selection of T^{**} . The subsequent linear regression analysis can yield optimal values of S_0 and β . In this way a precise estimation of

$\Delta T^{**} = T^{**} - T_{\text{IN}}$ is also possible, which is always a puzzling experimental problem. One should stress that the application of derivative-based analysis for the supplementary analysis is effective only for high-resolution experimental data.

2. Landau–de Gennes modeling

2.1. Nematic–smectic—A phase transition

Both de Gennes [56] and McMillan [57] have developed Landau theories of the N–SmA transition. Their original theories suggested that the N–SmA transition could be first or second order. Halperin *et al* [58] argued that the N–SmA transition can never be truly second order. However, later detailed work by Dasgupta and Halperin [59] predicted that in the regime of type-II superconductivity, the first-order N–SmA transition changes to a second-order N–SmA transition. The tricritical behavior of the N–SmA transition has been observed by changing the alkyl end chains [60], varying the concentration in binary mixtures [60–66], increasing the pressure [67] and increasing the electric field [68]. Other theoretical studies [69–72] also predicted the tricritical behavior of the N–SmA transition. In what follows we shall summarize the de Gennes model and its implications for dielectric permittivity. The layering in the SmA phase is characterized [5, 8] by the order parameter $\Psi(\mathbf{r}) = \Psi_0 \exp(-i\Psi)$, which is a complex scalar quantity whose modulus Ψ_0 is defined as the amplitude of a one-dimensional density wave characterized by the phase Ψ . 8OCB material is very polar due to the same cyano group being located at the terminal position. So one can conclude that the permanent dipole moment is parallel to the long rod-like axis. So we consider the SmA liquid crystals to be composed of strongly polar molecules. The external electric field induces a macroscopic polarization \mathbf{P} in the SmA phase. Then the free energy of the nematic phase close to the SmA phase in the presence of an applied electric field E will be the sum of the elastic energy of the nematic phase F_N , the fluctuating SmA energy F_A and electrostatic terms involving the polarization and the electric field F_E . Then the free energy can be written as:

$$F = \frac{1}{V} \int_V (F_N + F_A + F_E) dV \quad (17)$$

where

$$F_N = \frac{1}{2}K_1(\nabla \cdot \mathbf{n})^2 + \frac{1}{2}K_2(\mathbf{n} \cdot (\nabla \times \mathbf{n}))^2 + \frac{1}{2}K_3(\mathbf{n} \times (\nabla \times \mathbf{n}))^2,$$

$$F_A = \frac{1}{2}\alpha_1|\psi|^2 + \frac{1}{2}C_{\parallel}|\nabla_{\parallel}\psi|^2 + \frac{1}{2}C_{\perp}|(\nabla_{\perp} - iq_s\delta\mathbf{n}_{\perp})\psi|^2$$

$$F_E = \frac{1}{2}\gamma_1|\psi|^2P^2 + \frac{P_{\perp}^2}{2\varepsilon_0\chi_{\perp}} + \frac{P_{\parallel}^2}{2\varepsilon_0\chi_{\parallel}} - \mathbf{P} \cdot \mathbf{E}.$$

The elastic energy, as usual, contains three elastic constants K_1 (splay), K_2 (twist) and K_3 (bend), C_{\parallel} and C_{\perp} are components of a ‘mass tensor’ along and perpendicular to the unperturbed director \mathbf{n} , which lies along z direction. The coefficient $iq_s\delta\mathbf{n}_{\perp}$ takes into account so-called gauge

invariance. The polarization P is representative of the number of molecular dipoles aligned by the applied field. ε_0 is the vacuum permittivity. Parameters $\varepsilon_0\chi_{\parallel}$ and $\varepsilon_0\chi_{\perp}$ are the absolute dielectric susceptibilities. The parameter γ_1 is the anisotropy of the polarizability in the SmA phase. As usual $\alpha_1 = \alpha_0(T - T_{\text{NA}}^0)$, where T_{NA}^0 is the virtual transition temperature. All other coefficients, as well as α_0 , are assumed to be temperature independent. Now if the applied field is assumed to be in the x -direction parallel to the nematic axis, the nontrivial polarization P_x normal to the local director \mathbf{n} and of a modulation of Ψ in the y direction will be energetically favored. Then the nontrivial polarization must be derived by integrating out the thermal fluctuations of Ψ in the presence of the applied field E_x . In addition, the bend and twist are expelled at the N–SmA transition. In this case the free energy in Fourier space can be expressed as:

$$F = \frac{1}{2V} \sum_q [\alpha_1 + C_{\perp} q_{\perp}^2 + \gamma_1 P_x^2] \Psi_q \Psi_{-q} + \frac{P_x^2}{2\varepsilon_0\chi_{\perp}} - P_x E_x \quad (18)$$

where ψ_q is the Fourier transform of $\psi(r) = 1/V^{1/2} \sum_q \psi(\mathbf{q}) \exp(i\mathbf{q} \cdot \mathbf{r})$ and $\sum_q \rightarrow (V/(2\pi)^3) \int d^3\mathbf{q}$.

Now we define the effective free energy, which can be obtained by integrating out Ψ_q fluctuations in equation (18). Under the Gaussian approximation, the effective free energy f is just the ψ_q -independent part plus the free energy for the ψ_q -dependent part, which can be written as

$$e^{Vf/k_B T} = \int e^{-V F/k_B T} d\psi_q. \quad (19a)$$

After integration equation (19a) we get

$$f = \frac{P_x^2}{2\varepsilon_0\chi_{\perp}} - P_x E_x + \frac{1}{2} k_B T \int \frac{d^3\mathbf{q}}{2\pi^3} \ln G^{-1}(q, P_x) \quad (19b)$$

where $G^{-1}(q, P_x) = \alpha_1 + C_{\perp} q_{\perp}^2 + \gamma_1 P_x^2$.

Minimizing the free energy (19b) with respect to the polarization P_x leads to the equation of state for the polarization:

$$\frac{P_x}{\varepsilon_0\chi_{\perp}} - E_x + k_B T \int \frac{d^3\mathbf{q}}{2\pi^3} \frac{\gamma_1 P_x}{(\alpha_1 + C_{\perp} q_{\perp}^2 + \gamma_1 P_x^2)} = 0. \quad (20)$$

In the linear approximation (i.e. low field), the effective susceptibility in the nematic phase can be calculated from the last equation as:

$$\chi_{\text{N}} = \chi_{\perp} + AT + BT(T - T_{\text{NA}}^0)^{1/2} \quad (21)$$

where $A = -(\pi^2/2)\gamma_1 k_B \chi_{\perp}^2 \varepsilon_0 q_{\perp}$, $B = [(\pi^2/2)\gamma_1 \chi_{\perp}^2 \varepsilon_0 \alpha_0^{1/2} k_B / C_{\perp}^{3/2}] \tan^{-1}(q_{\perp}/\xi_{\perp})$ and $\xi_{\perp} = (\alpha_1/C_{\perp})^{1/2}$.

Hence the evolution of the dielectric constant in the nematic phase above the N–SmA phase transition can be written as:

$$\varepsilon'_{\text{N}}(T) = \varepsilon_{\text{N}}/\varepsilon_0 = 1 + \chi_{\perp} + AT + BT(T - T_{\text{NA}}^0)^{1/2}. \quad (22)$$

2.2. Isotropic–nematic transition

Owing to the inherent first-order nature of the I–N transition, experimental accessibility of the critical region and, therefore, the determination of the critical behavior has at best been difficult. Poggi *et al* [22], for example, obtained a critical exponent $\beta = 1/2$ (classical) for the I–N transition. Keyes [73, 74], however, has shown that $\beta = 1/4$ (tricritical) can also fit the data quite well. Keyes [73, 74] suggested that the critical exponents for quantities diverging towards temperature T^* , before being cut off by a first-order transition at $T_{\text{I–N}}$, should be the characteristic of a tricritical point. Concerning the specific heat, Anisimov *et al* [7] made a strong plea for the tricritical hypothesis, by fitting very precise specific heat measurements of MBBA and other compounds. Other theoretical studies [75–79] also predicted the tricritical behavior of the I–N transition. We intend to focus on the I–N transition in the vicinity of the tricritical point. Taking into account the relatively small value of the induced polarization, the Landau–de Gennes free energy in powers of Q_{ij} and P can be expressed as:

$$F = F_0 + \frac{1}{3} a Q_{ij} Q_{ij} - \frac{4}{9} b Q_{ij} Q_{jk} Q_{ki} + \frac{1}{9} c (Q_{ij} Q_{ij})^2 + \frac{4}{81} e (Q_{ij} Q_{ij})^3 + \frac{1}{2} L_1 \nabla_i Q_{jk} \nabla_i Q_{jk} + \frac{1}{2} L_2 \nabla_i Q_{ik} \nabla_j Q_{jk} + \frac{1}{2\chi_0} P^2 + \frac{1}{2} \eta Q_{ij} P_i P_j + \frac{1}{3} G_1 P_k P_n Q_{ki} Q_{nl} + \frac{1}{3} G_2 P_m P_m Q_{ij} Q_{ij} - P_i E_i \quad (23)$$

where F_0 is the free energy of the isotropic phase; χ_0 is the susceptibility; L_1 and L_2 are elastic constants; $a = a_0(T - T_{\text{I–N}}^*)$; and $T_{\text{I–N}}^*$ is the virtual transition temperature.

Further, the last equation can be simplified if one assumes that the polarization is aligned along the nematic director \bar{n} , i.e. $\mathbf{P} = (0, 0, P)$. We choose also $\mathbf{E} = (0, 0, E)$. The substitution of Q_{ij} and \mathbf{P} into the above equation leads to the free energy:

$$F = F_0 + \frac{1}{2} a S^2 - \frac{1}{3} b S^3 + \frac{1}{4} c S^4 + \frac{1}{6} e S^6 + \frac{1}{2} \left(L_1 + \frac{L_2}{2} \right) (\nabla S)^2 + \frac{1}{2\chi_0} P^2 - \frac{1}{2} \eta P^2 S + \frac{1}{2} G S^2 P^2 - PE \quad (24)$$

where $G = G_1 + G_2$.

For $E = 0$, $L_1 = 0$ and $L_2 = 0$, the above model dependence is adequate in reproducing a first order I–N transition with $b \neq 0$, $c > 0$ and $e = 0$. The latter condition assures a finite value of the order parameter and $b = 0$ and $c > 0$ indicates a critical point. If one presumes a weak first-order I–N transition near a critical point, the critical exponent β is found to have the classical value of $1/2$. As discussed above, the experimental situation (measured value of β) has led to the question whether the I–N transition is close to the tricritical point. In general, when two coefficients of the same symmetry vanish simultaneously we get a tricritical point. Coefficients $c = a = 0$ are for the tricritical point. As we have to consider a situation with $c = 0$, a stabilizing sixth-order term is added

with $e > 0$. Then the equation to determine the equilibrium value of S is [80]:

$$(S - S^{**})^4 + 4S^{**}(S - S^{**})^3 + 6(S^{**})^2(S - S^{**})^2 - (9a_0/4e)(T - T^{**}) = 0. \quad (25)$$

From which one get:

$$S - S^{**} \sim (T^{**} - T)^\beta \quad (26)$$

with $\beta = 1/4$. $S^{**} (= (b/4e)^{1/3})$ is the value of the metastable order parameter of the nematic phase and T^{**} is the metastable temperature of the nematic phase. Within the framework of the Landau theory one finds [28] that for $T < T^{**}$ ($b = 0$, $c = 0$): $G \sim (T^{**} - T)^{-\Delta}$, where $\Delta = 5/4$ is the gap exponent. Now for $E \neq 0$, minimizing the free energy with respect to the polarization P and substituting, we obtain the free energy density as a function of S as:

$$F = F_0^* + \frac{1}{2}aS^2 - \frac{1}{3}b^*S^3 + \frac{1}{4}c^*S^4 + \frac{1}{6}eS^6 + \frac{1}{2} \left(L_1 + \frac{L_2}{2} \right) (\nabla S)^2 - \frac{1}{2}\eta\chi_0^2 E^2 S + \frac{1}{2}\eta^2\chi_0^3 E^2 S^2 + \frac{1}{2}G\chi_0^2 E^2 S^2 \quad (27)$$

where the renormalized coefficients are $F_0^* = F_0 - E^2\chi_0/2$, $b^* = b + (3/2)\eta^3\chi_0^4 E^2 - 3\eta G\chi_0^3 E^2$ and $c^* = c - (3/2)G^2\chi_0^3 E^2 + 4G\eta^2\chi_0^4 E^2$.

Analysis of equation (27) shows that the influence of the external electric field on the polar smectic liquid crystals results in two main effects. First, the electric field produces a shift of the transition temperature T_{IN}^* which is proportional to the square of the electric field. Second, the external electric field induces weak orientational ordering ($S(E) = \eta\chi_0^2 E^2/2a$) in the isotropic phase. This nonzero value of the order parameter $S(E)$ is obtained to a first approximation (by taking $\partial F/\partial S = 0$).

The NDE denotes the change in the dielectric permittivity of a material that originates from the application of a strong static electric field E . Applying the same method as adopted by Mukherjee *et al* [80, 71], the NDE in the isotropic phase above the I–N transition to a first approximation ($b^* = 0$, $c^* = 0$, $e = 0$, $L_1 = L_2 = 0$) can be calculated as:

$$\varepsilon_{NDE} = \frac{\varepsilon(E) - \varepsilon(0)}{E^2} = \frac{U}{T - T_{IN}^*} \quad (28)$$

where $U = 2\eta\chi_0^2(\Delta\varepsilon_f)/3a_0$.

Similar to the procedure of section 2.1, the dielectric constant in the isotropic case is given by:

$$\varepsilon'_I(T) = \varepsilon_I/\varepsilon_0 = 1 + \chi_0 + A'T + B'T(T - T_{IN}^*)^{1/2} \quad (29)$$

where

$$A' = -(\pi^2/2)G\chi_0^3 q, \\ B' = ((\pi^2/2)\chi_0^2 a_0^{1/2} k_B / (L_1 + L_2/2)^{3/2}) \tan^{-1}(q/\xi_0), \\ \xi_0 = (a/(L_1 + L_2/2))^{1/2}.$$

The above analysis clearly indicates the tricritical behavior of the I–N and N–SmA transitions within the Landau–de Gennes theory based modeling.

3. Experimental details

This paper presents results of experimental studies in the rod-like liquid crystalline (LC) octyloxycyanobiphenyl (8OCB) with the Crystalline solid (Cr)–(310 K)–Smectic A–(340 K)–Nematic–(353.1 K)–Isotropic liquid phase sequence [8]. For the SmA–Cr transition $T_{SmA-Cr} \approx 322$ K is usually reported, hence the tested sample could be slightly supercooled. The 8OCB molecule is linked to a relatively large permanent dipole moment ($\sim 5D$), nearly parallel to the long axis of the molecule [8]. The tested compound was obtained thanks to the courtesy of Krzysztof Czupryński from Technical Military University (Warsaw, Poland). It was carefully purified to reach the lowest possible level of electric conductivity. Samples were always thoroughly degassed immediately prior to measurements.

The static dielectric permittivity and primary relaxation time evolution in rod-like thermotropic LC compounds has been tested over decades [5–12]. However, the successful implementation of distortion-sensitive analysis require features of experimental data that are hardly available so far. Among these are: (i) the essential minimization of parasitic artifacts which can scatter or bias experimental data, (ii) high resolution data, and (iii) a high ‘density’ of measurements, particularly in the vicinity of phase transitions.

The static dielectric permittivity ($\varepsilon'(T)$, $f = 10$ kHz) was measured via a Novocontrol Alpha analyzer with a permanent six-digit resolution. LC samples were located in two capacitors, with a macroscopic gap $d = 0.5$ mm, which is the basic scheme given in [81]. They were made from copper and completely gold coated, so samples were in contact only with gold, quartz and Teflon. The macroscopic gap made it possible to reduce/avoid surface effects and the influence of gas bubbles. Simultaneous measurements in two capacitors, with perpendicular (\perp) and parallel (\parallel) orientations of the molecules by the magnetic field ($B = 1.2$ T), were carried out at each temperature. The temperature was stabilized to ± 0.01 K. Consequently, a reliable estimation of the order parameter ($\Delta\varepsilon' = \varepsilon'_\parallel - \varepsilon'_\perp$) and the ‘diameter’ ($\varepsilon'_{\text{mean}} = (2/3)\varepsilon'_\perp + (1/3)\varepsilon'_\parallel$) directly from experimental data was possible. The analysis of the evolution of the static dielectric permittivity is particularly important for the results obtained, so the full set of $\varepsilon'(T)$ data is given in table A of the supplementary material (available at stacks.iop.org/JPhysCM/25/245105/mmedia). The rest of the experimental data is available on request (e-mail: sylwester.rzoska@gmail.com).

The nonlinear dielectric effect is defined as $\Delta\varepsilon^E/E^2 = (\varepsilon'(E) - \varepsilon'(E \rightarrow 0))/E^2$. The sample was placed in an analogous capacitor to that described above, but made from Invar. The total capacitance of the sample was $C \sim 100$ pF and the strong electric field induced changes $\Delta C^E \sim 5$ fF. The changes were detected with three-digit resolution. For LF NDE measurements a dual-field design [82, 83] with a weak electric probe field of $f_{\text{sampling}} \approx 20$ kHz and $V_{\text{peak-peak}} = 1$ V was implemented. Regarding the time scales: $\tau_{\text{sampling}} = 1/f_{\text{sampling}} \approx 50$ μs , whereas the longest life time of prenematic fluctuations in the isotropic phase was

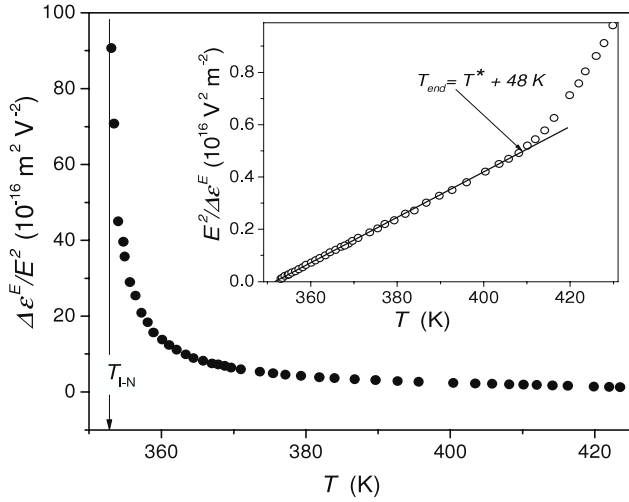


Figure 1. Results of LF NDE measurements in the isotropic phase of 8OCB. The inset shows the reciprocal of experimental data, proving the validity of the simple LdG equations (1) and (30), with $A_{\text{NDE}} = 108$ ($10^{-16} \text{ m}^2 \text{ V}^{-2} \text{ K}$), taken from the slope of the line. The value of the discontinuity was determined as $\Delta T^* = T_{\text{IN}} - T^* \approx 1.2 \text{ K}$, assuming $E^2/\Delta\epsilon^E = 0$ for $T = T^*$, $T^C = T_{\text{IN}}$.

$\tau_{\text{fluct.}}(T_{\text{IN}}) \approx 1 \mu\text{s}$ [8, 26]. The strong electric field was used in the form of 10 ms duration DC pulses, whose voltage was changed from $V = 200$ to 800 V (for $d = 0.5 \text{ mm}$) to control the validity of the $\Delta\epsilon^E \propto E^2$ condition.

The primary relaxation time was determined from the dielectric loss curve ($\epsilon''(f)$) via the $\tau = 1/2\pi f_{\text{peak}}$ condition. The primary relaxation time estimated in this way is proportional to the one obtained via Havriliak–Negami (HN) function fitting of the dielectric loss curve. However, due to the applied procedure, one avoids a significant error associated with the multiparameter HN fitting. The loss curves were taken from the spectrum obtained using a BDS 80 Novocontrol spectrometer for a non-oriented sample placed in a gold-coated capacitor with a $d = 0.1 \text{ mm}$ gap and $V_{\text{p-p}} = 0.2 \text{ V}$ measuring field.

Supplementary heat capacity measurements were obtained using the differential scanning calorimeter DSC-Q2000 from TA-Instruments working in a modulated mode (MDSC). In our work, the experimental conditions (temperature amplitude and oscillation period) were adjusted to obtain only the real part (the static part) of the complex heat capacity. A more detailed description of the MDSC technique can be found elsewhere [39, 84]. Experiments were performed on cooling from the isotropic phase down to the SmA mesophase and on heating up to the isotropic phase, all runs made at 0.01 K min^{-1} . The modulation parameters (temperature amplitude and oscillation period) were $\pm 0.035 \text{ K}$ and 25 s .

4. Results and discussion

Figure 1 shows results of the low-frequency ‘nonlinear static dielectric permittivity’ (LF NDE) measurements in the isotropic phase of 8OCB. On approaching the clearing temperature (I–N transition), a strong increase of LF NDE

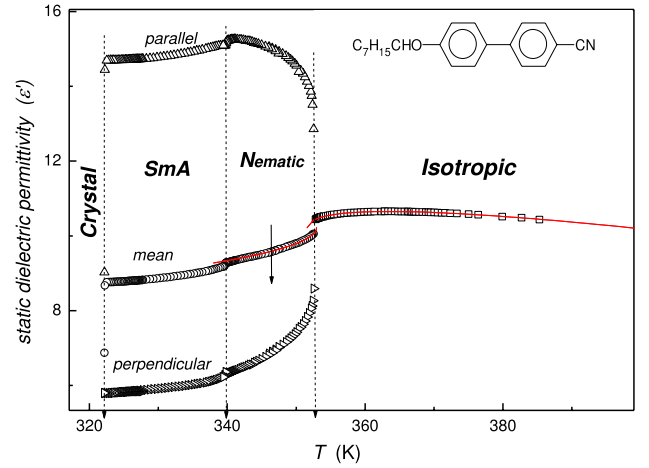


Figure 2. The temperature evolution of the static dielectric permittivity in 8OCB. Solid curves are given by equations (3) and (31), with the parameters given in table 1.

occurs. It can be described by a dependence in fair agreement with equations (1) and (28):

$$(\text{LFNDE})^{-1} = E^2/\Delta\epsilon^E = -A_{\text{NDE}}^{-1}T^* + A_{\text{NDE}}^{-1}T, \quad (30)$$

for $T > T^C$.

The plot based on equation (30) enables a simple validation of the exponent $\gamma = 1$ and the precise estimation of the virtual critical temperature T^* via the condition $E^2/\Delta\epsilon^E(T^*) = 0$. It is noteworthy that transient grating optical Kerr effect studies in the isotropic phase of 5CB led to the conclusion that, at $T_{\text{end}} \approx T^C + 40 \text{ K}$, prenematic fluctuations reduce to two to three molecules and are subsequently not detectable by methods directly coupled to fluctuations [85, 86]. This can be recognized as the reason for the distortion from equation (30) for $T > T_{\text{end}} \approx T^C + 48 \text{ K}$ (figure 1).

The evolution of the pretransitional anomaly of the ‘linear’ static dielectric permittivity $\epsilon'(T)$ is qualitatively different from LF NDE, as shown in figure 2 and in more detail in figure 3. The pretransitional behavior is well represented via equations (3) and (31), as shown by the solid curves in figures 2 and 3. In LC mesophases the static dielectric permittivity splits into the perpendicular (ϵ'_{\perp}) and the parallel (ϵ'_{\parallel}) components due to the rod-like geometry of the molecule (figure 2).

To compare the behavior in the isotropic phase and LC mesophases, the mean permittivity, $\epsilon'_{\text{mean}} = (2/3)\epsilon'_{\perp} + (1/3)\epsilon'_{\parallel}$, has been tested for $T < T^C = T_{\text{IN}}$. Its evolution can be given by [13]:

$$\epsilon'_{\text{mean}}(T) = \epsilon^{**} + a_{\text{mean}} \left(\frac{T^{**} - T}{T^{**}} \right) + A_{\text{mean}} \left(\frac{T^{**} - T}{T^{**}} \right)^{1-\alpha} \quad \text{for } T < T_{\text{IN}}. \quad (31)$$

To reduce the uncertainty in the multiparameter fitting of $\epsilon'(T) = \epsilon'_{\text{iso}}(T)$ and $\epsilon'_{\text{mean}}(T)$, the initial value of ΔT^* was taken from LF NDE measurements, and estimations of the remaining parameters were supported by the derivative-based

Table 1. Results of fitting experimental dependences for the dielectric permittivity in the isotropic liquid and for the mean permittivity using equations (3), (31)–(37).

Phase transition	$\varepsilon^*, \varepsilon^{**}$	ΔT (K)	a (K ⁻¹)	A (K ⁻¹)	Exponent α
I–N (<i>isotropic</i>)	10.20	1.25	–13.36	4.9	0.51
N–I (<i>nematic</i>)	10.35	0.55	11.88	–6.89	0.48
N–SmA (<i>nematic</i>)	9.27	$\Delta T < 0.1$	8.43	2.96	0.2
SmA–N (<i>smectic</i>)	9.21	$\Delta T < 0.1$	7.94	–10.26	0.2

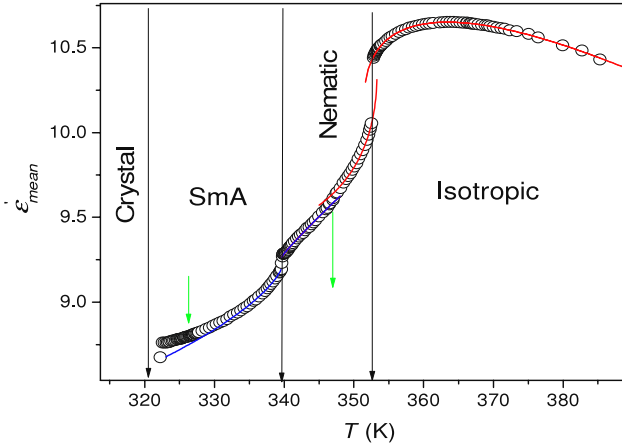


Figure 3. The temperature evolution of the mean static dielectric permittivity in subsequent phases of 80CB. Green arrows indicate ‘fluid–fluid crossovers’ manifesting in figure 4.

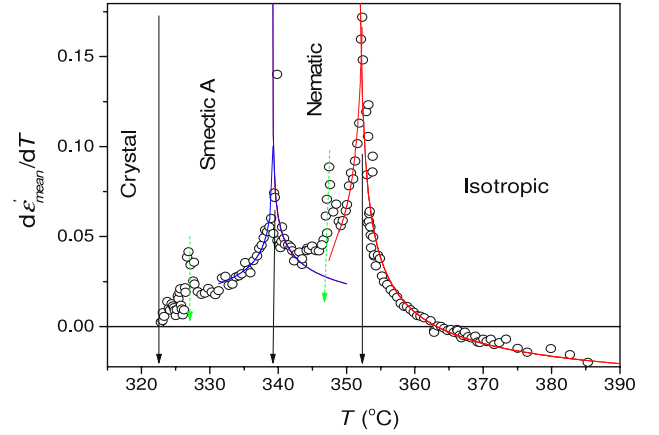


Figure 4. Results of the derivative-based, distortion-sensitive analysis of the mean dielectric permittivity in 80CB, based on data from figure 3. Dashed arrows show a subsequent phase transition, while solid, small (green) arrows indicate ‘crossover transitions’. Blue curves (equations (36) and (37)) are for the N–SmA transition and red curves for I–N transition, with parameters collected in table 1.

analysis:

$$\frac{d\varepsilon'_{\text{mean}}}{dT} = a_{\text{mean}} + (1 - \alpha)A_{\text{mean}} \left(\frac{T^{**} - T}{T^{**}} \right)^{-\alpha} \quad (32)$$

$$\frac{d\varepsilon'_{\text{Iso}}}{dT} = a_{\text{Iso}} + (1 - \alpha)A_{\text{Iso}} \left(\frac{T - T^*}{T^*} \right)^{-\alpha} \quad (33)$$

Values of the fitted parameters are collected in table 1. To represent the pretransitional anomaly for the N–SmA transition on cooling, the relation parallel to equation (3) with an arbitrary power exponent $\phi = 1 - \alpha$ was used, namely:

$$\varepsilon'_N = \varepsilon_N^* + a_N(T - T_N^*) + A_N(T - T_N^*)^{1-\alpha} \quad (34)$$

for $T > T_{N-\text{SmA}}$

$$\varepsilon'_{\text{SmA}} = \varepsilon_{\text{SmA}}^* + a_{\text{SmA}}(T_{\text{SmA}}^* - T) + A_N(T_{\text{SmA}}^* - T)^{1-\alpha} \quad (35)$$

for $T < T_{N-\text{SmA}}$

and

$$\frac{d\varepsilon'_N}{dT} = a_N + (1 - \alpha')A_N(T - T_N^*)^{-\alpha} \quad (36)$$

for $T > T_{N-\text{SmA}}$

$$\frac{d\varepsilon'_{\text{SmA}}}{dT} = a_{\text{SmA}} + (1 - \alpha')A_{\text{SmA}}(T_{\text{SmA}}^* - T)^{-\alpha} \quad (37)$$

for $T < T_{N-\text{SmA}}$.

Results of fitting data via equations (31)–(37) are shown in figures 2–4 and table 1. It is noteworthy that for the N–SmA transition the application of equations (22) and (34) yields approximately the same values of relevant parameters, due

to the small range of temperature, so within the experimental error $BT \approx A_N = \text{const}$. The application of derivative-based analysis reduces the number of fitted parameters, anomalies are more pronounced and domains of validity of the given critical-like behavior are clearly indicated prior to the final fitting. Such analysis can also bring to light even subtle features, due to its distortion-sensitive nature. These features are clearly visible in figure 4, which reveals that neither nematic nor SmA mesophases are uniform and ‘weak fluid–fluid crossovers’ associated with the approach of the subsequent mesophase appear. Surprisingly, this takes place also on approaching the crystallization. The obtained values of the specific heat exponent α from $\varepsilon'(T)$ and $d\varepsilon'(T)/dT$ evolutions are in fair agreement with ones obtained from heat capacity measurements [7–9, 37–39]. However, hallmarks for the mentioned crossovers are absent in the heat capacity scan, as shown in figure 5, despite the fact that one can assume $C_P \propto d\varepsilon'/T$ (see the above LdG model analysis and [87]).

This may be associated with the fact that ‘crossovers’ are associated solely with structural changes related to different dipole–dipole arrangements. Nevertheless, the results presented in figure 4 can significantly facilitate fitting of $C_P(T)$ anomalies, since they indicate domains of dominance for the given pretransitional anomaly. These estimations have been employed for the results presented in figure 5. It is notable that the correction-to-scaling term could

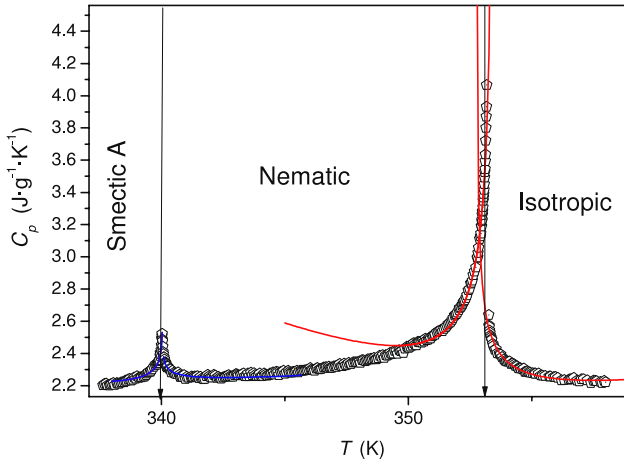


Figure 5. Heat capacity behavior in 8OCB. To describe pretransitional anomalies for the I–N (in red) and N–SmA (in blue) transitions equation (8) was employed. The influence of the correction-to-scaling term was neglected and domains of dominance for pretransitional effects from figure 4 were taken into account.

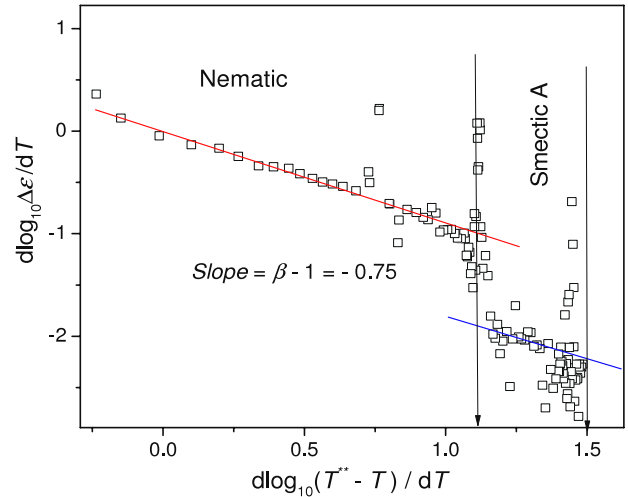


Figure 6. Results of the derivative-based analysis of data from figure 1, in the isotropic and in LC mesophases of 8OCB on a scale showing the critical-like behavior in equation (38). The value of the exponent is $\beta \approx 14$.

be neglected since its influence is important solely for the clearly non-classical case and when the domain is far away from the critical point [7].

One of the most fundamental properties characterizing a continuous phase transition is the order parameter. Probably the most popular experimental metric of the order parameter can be associated with the static dielectric permittivity:

$$S(T) \propto \varepsilon_{\parallel} - \varepsilon_{\perp} = \Delta\varepsilon^{**} + B(T^{**} - T)^{\beta} \quad (38)$$

where T^{**} is the extrapolated terminal temperature of the supercooled nematic phase, $\Delta\varepsilon^{**}$ is a constant and $T < T_{NI} = T^{**} - \Delta T^{**}$.

The supporting, derivative-based analysis, was also employed:

$$\frac{d(\Delta\varepsilon)}{dT} = B\beta(T^{**} - T)^{\beta-1}. \quad (39)$$

Results of such analysis are shown in figure 6. It shows clear evidence for $\beta = 0.25 \pm 0.03$, with distortions in the immediate vicinity of phase transitions. The transition from the nematic to the SmA mesophase seems to lead solely to the shift of the amplitude B .

The question arises if pretransitional anomalies as well as hallmarks of the mentioned ‘weak crossover fluid–fluid transitions’ within the mesophases can be detected also for dynamic properties. This issue was tested via the analysis of the temperature evolution of the primary relaxation time.

It is noteworthy that the distribution of relaxation times, which can be detected from the shape of the loss curve related to the primary relaxation time, is clearly non-Debye, as shown in recent in-depth analysis. The broadening of loss curves is asymmetric and particularly strong near the I–N transition [17, 54]. Consequently, the optimal representation is via the Havriliak–Negami (HN) function or the Jonsher approach [88]. The parameterization via the Cole–Cole (CC) or Cole–Davidson (CD) function, often used in the past, is clearly inadequate. The CC function is

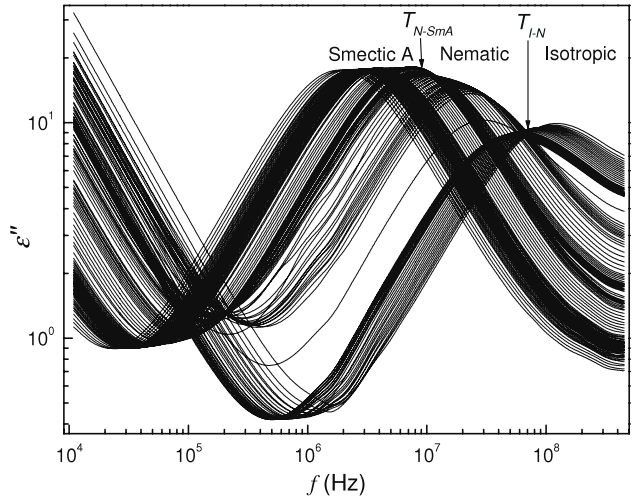


Figure 7. Dielectric loss curves in the isotropic liquid and mesophases of 8OCB.

associated with the symmetric broadening of the loss curve and the CD function assumes Debye-type behavior for the high-frequency wing of the loss curve. In this paper the dielectric relaxation time was estimated via $\tau = 1/2\pi f_{\text{peak}}$, which is proportional to the relaxation time estimated from HN function fitting [88]. However, determining the relaxation time from the coordinates of the peak of the loss curve is not influenced by any noticeable error related to the multiparameter fitting [88]. The up-to-date discussion of the distribution of relaxation time in rod-like LC compounds can be found in [17, 54]. The obtained temperature evolution of primary relaxation times is shown in figure 8.

For technical reasons it was not possible to carry out high-frequency BDS measurements under a strong magnetic field, so in the LC mesophase tests were carried out in a non-oriented sample. The obtained behavior of the primary relaxation time, shown in figure 8, seems to follow

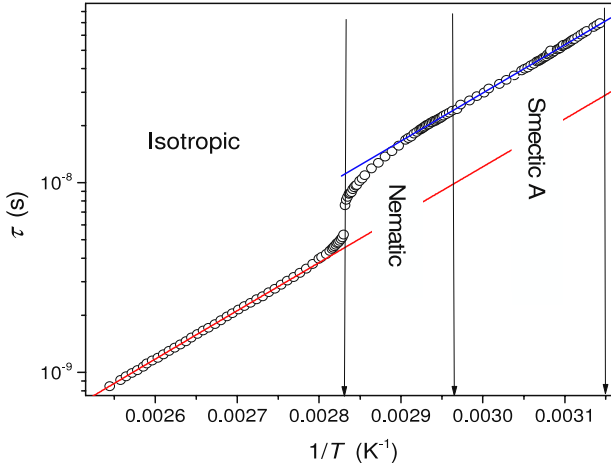


Figure 8. The Arrhenius plot of the evolution of dielectric relaxation times in isotropic and liquid crystalline 80CB. Solid curves plot the ‘critical-like’ equation (11) with parameters taken from figure 7 (power exponent $\phi = 8.5$ and $T_C = 171$ K).

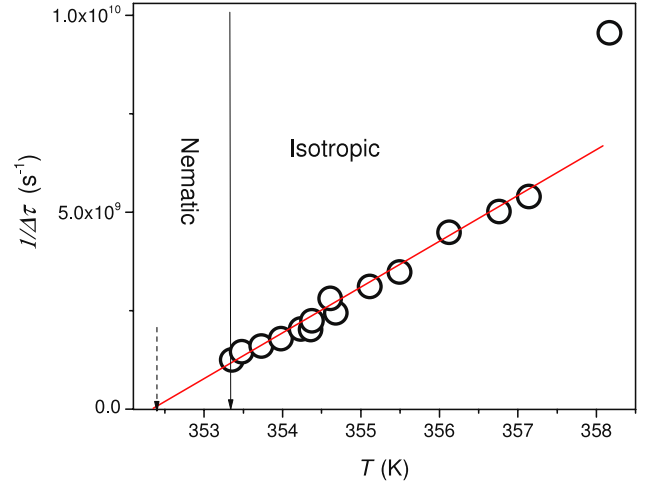


Figure 10. The plot showing the form of the temperature evolution of the excess relaxation time in the isotropic phase, in the immediate vicinity of the I–N transition; $\Delta\tau = \tau - \tau_{bckg}$ and $\Delta\tau \propto 1/(T - T^*)$, where τ_{bckg} describes the extrapolated evolution of $\tau(T)$ remote from the clearing point, given by equation (11) with parameters estimated from figure 9.

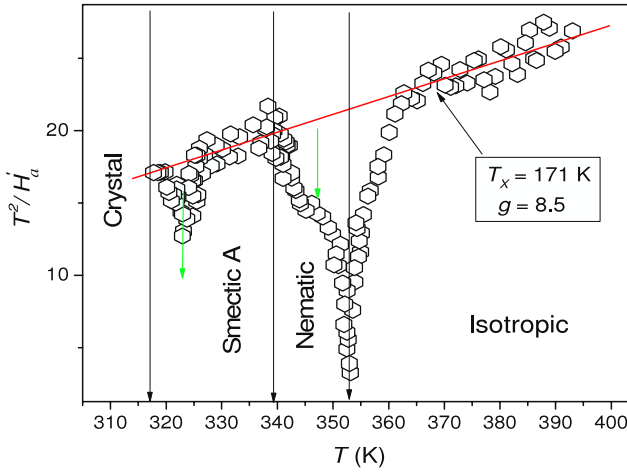


Figure 9. The linearized, derivative-based transformation of dielectric relaxation data, focused on the validity of the critical-like relation (11) in the description of dynamics in 80CB. All parameters given in the figure were determined from the linear regression analysis via equation (35).

the Arrhenius behavior $\tau(T) = \tau_0 \exp(E_a/RT)$, $E_a = \text{const}$. However, the distortion-sensitive analysis, whose results are presented in figure 9, shows that the evolution is clearly non-Arrhenius and can be parameterized by equation (11). In figure 9, linear domains indicate the regions of validity of equation (11). The subsequent linear regression can yield optimal values of the fundamental parameters T_X and ϕ . The obtained value of the exponent $\phi \approx 8.5$ coincides fairly well with the universal behavior of uniaxial glass forming systems at the glass transition [14–16], but here it occurs also in the high-temperature domain. It was possible to estimate the hypothetical glass transition temperature for $T_g \approx 185$ K, calculated as $\tau(T_g) = 100$ s [88]. Similarly to figure 4, there is a notable appearance of ‘fluid–fluid’ crossover transitions’ within the mesophases in figure 9.

Figures 9 and 10 show that in the isotropic phase, in the immediate vicinity of T_{IN} , an extra slowing down occurs. As shown in figure 10 it can be well described via the relation:

$$\Delta\tau(T) = \tau_{bckg}(T) - \tau(T) \propto \frac{1}{T - T^*}. \quad (40)$$

It is worth stressing that the values of ΔT^* obtained from figure 9 are in fair agreement with that determined from *LF NDE* studies.

5. Conclusions

This paper gives the results of studies on the static dielectric properties in the I, N and SmA phases of 80CB, one of the most ‘classical’ rod-like LC compounds, combined with measurements of low-frequency nonlinear dielectric effects and the heat capacity. Due to the implementation of the distortion-sensitive and derivative-based analysis the so-far lacking evidence for pretransitional anomalies of the static dielectric permittivity for both I–N and I–SmA transitions has been obtained. For the I–N transition, the obtained behavior agrees with the tricritical hypothesis: a value of the order parameter exponent $\beta \approx 1/4$, a specific heat exponent $\alpha \approx 1/2$ and a ratio of discontinuities $\Delta T^{**}/\Delta T^* \approx 1/2$ [86] (see tables 1 and 2). Noteworthy is the validation of the approximate scaling relation $A^+/A^- \approx 1 - 4\alpha$ [89–92].

Regarding the N–SmA transition, the obtained value of the exponent $\alpha \approx 0.2$ from the analysis of $\epsilon'_{\text{mean}}(T)$ and $d\epsilon'_{\text{mean}}(T)/dT$ evolutions agrees well with estimations from heat capacity measurements ($C_P(T)$). The value of the exponent is neither tricritical ($\alpha = 1/2$) nor the ‘non-classical’ 3D XY Ising universality class ($\alpha \approx -0.07$). However, the exponent $\beta \approx 1/4$, except in the immediate vicinity of the transition. Generally, the tricritical point is linked to the connection of the three curves of the critical point [93]. In

Table 2. Results of fitting experimental dependences of the heat capacity in the isotropic liquid and in the nematic and SmA phases respectively.

Phase transition	$b_{IN}, b_{NI}, b_{NA}, b_{AN}$	$\Delta T^*, \Delta T^{**}$ (K)	$a_{IN}, a_{NI}, a_{NA}, a_{AN}$	$A_{IN}, A_{NI}, A_{NA}, A_{AN}$	Exponent α
I–N (<i>isotropic</i>)	1.92	0.50	7.5	0.024	0.50
N–I (<i>nematic</i>)	1.46	0.25	24.5	0.057	0.50
N–SmA (<i>nematic</i>)	1.99	>0.04	4.67	0.154	0.15
SmA–N (<i>smectic</i>)	2.02	>0.04	3.72	0.088	0.16

the case of the symmetrical tricriticality, to which LC systems belong, it manifests via the transition from the curve linked to discontinuous phase transitions to continuous ones [93, 7]. The obtained value of the exponent may suggest that, depending on molecular features, different LC compounds are located at different loci along the mentioned curves. As the confirmation, studies of the heat capacity/specific heat in LC mixtures or in homologous series of LC compounds may serve [8–12]. Important may appear lacking so far studies under various hydrostatic pressures, hypothetically yielding different values of exponents α .

We must also conclude from the experiments for many 8OCB compounds that either the Gaussian approximation is insufficient to describe the NA transition or the LdG model has to be modified. The LdG model can be improved upon by using a perturbation calculation beyond Gaussian. Thus this disagreement can be explained by taking these effects into account. However, such calculations are beyond the scope of this paper. Worth stressing is the evidence of ‘crossover transitions’ within the LC mesophase. For instance, the nematic phase splits into parts dominated by pretransitional fluctuations associated with the I–N and N–SmA transitions. This fact may be important in the analysis of experimental data, since fitting in improperly selected temperature domains can lead to overestimated and effective values of exponents.

Regarding the dynamics, the evolution of the primary relaxation time is non-Arrhenius and critical-like. Also worth stressing is the novel pretransitional anomaly of the primary relaxation time in the isotropic phase, linked to the hypothetical continuous phase transition at T^* . We would also like to indicate an unsolved problem appearing when comparing values of discontinuities ΔT^* and ΔT^{**} linked to the I–N transition determined from $\varepsilon'(T)$, LF NDE, CME, KE and $C_p(T)$ studies. For the latter these values are about 50% smaller: (see tables 1 and 2 and compare results in [8–12, 38–40]).

In conclusion, the results presented show the strong dominance of the pretransitional effects in the isotropic liquid and mesophases of 8OCB, a model LC rod-like compound. They also show the fundamental importance of the supplementary distortion-sensitive analysis in giving reliable insights.

Acknowledgments

SJR and ADR were supported by grant no. 2011/03/B/ST3/02352 from the National Centre for Science (NCN, Poland, grant holder: S J Rzoska). DOL is grateful for financial support from the MICINN project MAT2009-14636-C03-02.

References

- [1] de Gennes P G 1992 *Soft Matter (Nobel Lecture)*, *Science* **24** 495
de Gennes P G 1992 *Angewandte Chemie Int. Ed.* **31** 842 (English)
- [2] Jones R A L 2002 *Introduction to Soft Matter* (New York: Oxford University Press)
- [3] Hamley I W 2007 *Introduction to Soft Matter: Synthetic and Biological Self-Assembling Materials* (New York: Wiley)
- [4] Mezzenga R, Schurtenberger P, Burbridge A and Michel M 2005 *Nature Mater.* **5** 729
- [5] de Gennes P G 1974 *The Physics of Liquid Crystals* (New York: Oxford University Press)
de Gennes P G and Prost J 1995 *The Physics of Liquid Crystals* (New York: Oxford University Press)
- [6] Vertogen G and de Jeu W H 1988 *Thermotropic Liquid Crystals, Fundamentals (Springer Series in Chemical Physics Band) vol 45* (Berlin: Springer)
- [7] Anisimov M A 1991 *Critical Phenomena in Liquids and Liquid Crystals* (Reading, MA: Gordon and Breach)
- [8] Demus D, Goodby J, Gray G W, Spiess H W and Vill V (ed) 1998 and 2008 *Handbook of Liquid Crystals, Vol 1: Fundamentals* (Berlin: Springer)
- [9] Chandrasekhar S 1994 *Liquid Crystals* (Cambridge: Cambridge University Press)
- [10] Singh S 2002 *Liquid Crystals: Fundamentals* (Singapore: World Scientific)
- [11] Dunmurr D, Fukuda A and Luckhurst G R (ed) 2007 *Physical Properties of Liquid Crystals: Nematics* (London: Inst. Engn. and Technol)
- [12] Kumar S 2011 *Liquid Crystals: Experimental Studies of Physical Properties and Phase Transitions* (Cambridge: Cambridge University Press)
- [13] Rzoska S J, Ziolo J, Sułkowski W, Jądzyn J and Czechowski G 2001 *Phys. Rev. E* **64** 052701
- [14] Drozd-Rzoska A and Rzoska S J 2006 *Phys. Rev. E* **73** 041502
- [15] Drozd-Rzoska A, Rzoska S J and Paluch M 2009 *J. Chem. Phys.* **129** 184509
- [16] Drozd-Rzoska A 2009 *J. Chem. Phys.* **130** 234910
- [17] Rzoska S J, Pawlus S and Czuprynski K 2011 *Phys. Rev. E* **84** 031710
- [18] Martinez-Garcia J C, Martinez-Garcia J and Rzoska S J 2012 *J. Chem. Phys.* **137** 064501
- [19] de Gennes P G 1969 *Phys. Lett. A* **30** 454
- [20] Stinson T W and Litster J D 1973 *Phys. Rev. Lett.* **30** 688
- [21] Madhusudana N V and Chandrasekhar S 1973 *Pramana* **1** 12
- [22] Poggi Y, Atten P and Filippini J C 1976 *Mol. Cryst. Liq. Cryst.* **37** 1
- [23] Wong G K L and Shen Y R 1974 *Phys. Rev. A* **10** 1277
- [24] Bendler J 1977 *Mol. Cryst. Liq. Cryst.* **38** 19
- [25] Coles H J 1978 *Mol. Cryst. Liq. Cryst.* **41** 231
- [26] Yamamoto R, Isihar S, Hayakawa S and Morimoto K 1978 *Phys. Lett. A* **69** 276
- [27] Kolynsky P V and Jennings B R 1980 *Mol. Phys.* **40** 979
- [28] Keyes P H and Daniels W B 1979 *J. Physique* **40** 380
- [29] Poulligny B, Sein E and Lalanne J R 1980 *Phys. Rev. A* **24** 1528

- [30] Drozd-Rzoska A, Rzoska S J and Ziolo J 2000 *Phys. Rev. E* **61** 5349
- [31] Drozd-Rzoska A, Rzoska S J and Czupryński K 2000 *Phys. Rev. E* **61** 5355
- [32] Thoen J and Menu G 1983 *Mol. Cryst. Liq. Cryst.* **97** 163
- [33] Drozd-Rzoska A, Rzoska S J and Ziolo J 1996 *Phys. Rev. E* **54** 6452
- [34] Drozd-Rzoska A, Pawlus S and Rzoska S J 2001 *Phys. Rev. E* **64** 051701
- [35] Birgeneau R J, Garland C W, Kasting G B and Ocko B M 1981 *Phys. Rev. A* **24** 2624
- [36] Żywociński A 2003 *J. Phys. Chem. B* **107** 9491
- [37] Stine K J and Garland C W 1989 *Phys. Rev. A* **39** 1482
- [38] Cordoyiannis G, Tripathi C S P, Glorieux C and Thoen J 2010 *Phys. Rev. E* **82** 031707
- [39] Cusmin P, Fuente M R, Salud J, Perez-Jubindo M A, Diez-Berart S and Lopez D O 2007 *J. Phys. Chem. B* **200** 8974
- [40] Sebastián N, López D O, Diez-Berart S, Rosario de la Fuente M, Salud J, Pérez-Jubindo M A and Ros M B 2011 *Materials* **4** 1632
- [41] Haller M 1975 *Prog. Solid State Chem.* **10** 103
- [42] Urban S and Würflinger A 1997 *Advances in Chemical Physics* vol XCVIII, ed I Prigogine and A Rice (New York: Wiley) pp 143–216
- [43] Urban S, Gestblom B, Kuczyński W, Pawlus S and Würflinger A 2003 *Phys. Chem. Chem. Phys.* **5** 924
- [44] Kumar Das M, Sarkar G, Das B, Rai R and Sinha N 2012 *J. Phys.: Condens. Matter.* **24** 115101
- [45] Tough R J A and Bradshaw M J 1983 *J. Physique* **44** 447
- [46] Simões M and Simeão D S 2006 *Phys. Rev. E* **74** 051701
- [47] Sigdel K P and Iannacchione G S 2010 *Phys. Rev. E* **82** 051702
- [48] Roshi A, Iannacchione G S, Clegg P S, Birgeneau R J and Neubert M E 2005 *Phys. Rev. E* **72** 051716
- [49] Rzoska S J and Zhelezny V (ed) 2004 *Nonlinear Dielectric Phenomena in Complex Liquids (NATO Sci. Series II)* vol 157 (Dordrecht: Kluwer)
- [50] Diogo A C and Martins A F 1982 *J. Physique (Paris)* **43** 779
- [51] Buivydas M, Gouda F, Matuszczyk M and Lagerwall S T 1998 *Proc. SPIE* **3318** 94
- [52] Zeller H R 1982 *Phys. Rev. Lett.* **48** 334
- [53] Schadt H and Zeller H R 1982 *Phys. Rev. A* **26** 2940
- [54] Martinez-Garcia J C, Tamarit J Ll and Rzoska S J 2011 *J. Chem. Phys.* **134** 144505
- [55] Drozd-Rzoska A and Rzoska S J 2010 Anomalous decoupling of the dc conductivity and the structural relaxation time in the isotropic phase of a rod-like liquid crystalline compound *Metastable Systems under Pressure (NATO Sci. Series II)* (Berlin: Springer)
- [56] de Gennes P G 1972 *Solid State Commun.* **10** 753
- [57] McMillan W 1971 *Phys. Rev. A* **4** 1238
- [58] Halperin B I, Lubensky T C and Ma S K 1974 *Phys. Rev. Lett.* **32** 292
- [59] Dasgupta S and Halperin B I 1981 *Phys. Rev. Lett.* **47** 1556
- [60] Doane J W, Parker R S, Cvikl B, Johnson D L and Fishel D L 1972 *Phys. Rev. Lett.* **28** 1694
- [61] Thoen J, Marynissen H and Van Dael W 1983 *Phys. Rev. Lett.* **52** 204
- [62] Marynissen H, Thoen J and Van Dael W 1983 *Mol. Cryst. Liq. Cryst.* **124** 195
- [63] Garland C W, Nounesis G and Stine K J 1989 *Phys. Rev. A* **39** 4919
- [64] Johnson D L, Maze C, Oppenheim E and Reynolds R 1975 *Phys. Rev. Lett.* **34** 1143
- [65] Dasgupta S and Roy S K 2000 *Phys. Lett. A* **306** 235
- [66] Denolf K, Roie B V, Glorieux C and Thoen J 2006 *Phys. Rev. Lett.* **97** 107801
- [67] Mckee T J and McColl J R 1975 *Phys. Rev. Lett.* **34** 1076
- [68] Lelidis I and Durand G 1994 *Phys. Rev. Lett.* **73** 672
- [69] Alben R 1973 *Solid State Commun.* **13** 1783
- [70] Longa L 1986 *J. Chem. Phys.* **85** 2974
- [71] Mukherjee P K 2002 *J. Chem. Phys.* **116** 9531
- [72] Mukherjee P K and Sasmal S 2011 *Phase Transit.* **84** 110
- [73] Keyes P H 1978 *Phys. Lett. A* **67** 132
- [74] Keyes P H and Shane J R 1979 *Phys. Rev. Lett.* **42** 722
- [75] Buka A and de Jeu W H 1982 *J. Physique* **43** 361
- [76] Gramsbergen E F, Longa L and de Jeu W H 1986 *Phys. Rep.* **135** 195
- [77] Mukherjee P K 1997 *Mod. Phys. Lett.* **11** 107
- [78] Syed I M, Pereec V, Petshek R G and Rosenblatt C 2003 *Phys. Rev. E* **67** 011704
- [79] Lenart V M, Gomez S L, Bechtold I H, Neto A M F and Salinas S R 2012 *Eur. Phys. J. E* **35** 14
- [80] Mukherjee P K 1998 *J. Phys.: Condens. Matter.* **10** 9191
- [81] Rzoska S J, Chrapeć J and Ziolo J 1988 *J. Phys. Chem.* **92** 2064
- [82] Drozd-Rzoska A, Rzoska S J and Ziolo J 1996 *Liq. Cryst.* **21** 273
- [83] Rzoska S J and Drozd-Rzoska A 2012 *J. Phys.: Condens. Matter.* **24** 035101
- [84] Sied M B, Salud J, López D O, Barrio M and Tamarit J Ll 2002 *Phys. Chem. Chem. Phys.* **4** 2587
- [85] Torre R 2007 *Time Resolved Spectroscopy in Complex Liquids* (Berlin: Springer)
- [86] Cang H, Li J, Novikov V N and Fayer M D 2003 *J. Chem. Phys.* **119** 10421
- [87] Mistura L 1973 *J. Chem. Phys.* **59** 4563
- [88] Kremer F and Schoenhals A 2003 *Broad Band Dielectric Spectroscopy* (Berlin: Springer)
- [89] Stine K J and Garland C W 1989 *Phys. Rev. A* **39** 3148
- [90] Barmatz P, Hohenberg P C and Kornblit C 1975 *Phys. Rev. B* **12** 1947
- [91] Hohenberg P C, Aharony A, Halperin B I and Siggia E D 1976 *Phys. Rev. B* **13** 2986
- [92] Aharony A and Hohenberg P C 1976 *Phys. Rev. B* **13** 3081
- [93] Wheeler J C 1984 *J. Chem. Phys.* **18** 3635